Integral of solid spherical harmonic expansions at grid cells residing on undulated surfaces

Blažej Bucha

Department of Theoretical Geodesy and Geoinformatics
Slovak University of Technology in Bratislava
blazej.bucha@stuba.sk

The X. Hotine–Marussi Symposium, Milan

Motivation

What is the integral

$$\boxed{\tilde{V}_{ij} = \frac{1}{\Delta\sigma_{ij}} \int\limits_{\lambda=\lambda_j}^{\lambda_{j+1}} \int\limits_{\theta=\theta_i}^{\theta_{i+1}} V\left(r(\theta, \lambda), \theta, \lambda\right) \, \sin\theta \, \mathrm{d}\theta \, \mathrm{d}\lambda}$$

Motivation

What is the integral

$$\boxed{\tilde{V}_{ij} = \frac{1}{\Delta\sigma_{ij}} \int\limits_{\lambda=\lambda_j}^{\lambda_{j+1}} \int\limits_{\theta=\theta_i}^{\theta_{i+1}} V\left(r(\theta,\lambda), \theta, \lambda\right) \, \sin\theta \, \mathrm{d}\theta \, \mathrm{d}\lambda}$$

of

$$V(r,\theta,\lambda) = \frac{G\,M}{R} \sum_{n=0}^{N_1} \left(\frac{R}{r(\theta,\lambda)}\right)^{n+1} \sum_{m=0}^{n} \sum_{l=0}^{1} \bar{V}_{lnm} \, \bar{Y}_{lnm}(\theta,\lambda)?$$

Motivation

Undulated cell with variable $r(\theta, \lambda)$:

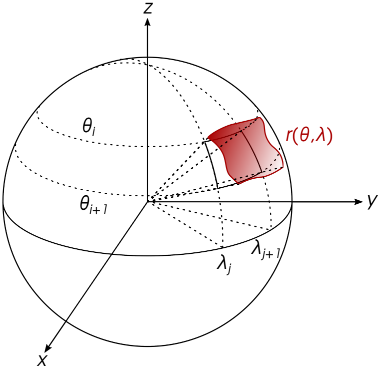

Figure: Undulated cell

Motivation

Undulated cell with variable $r(\theta, \lambda)$:

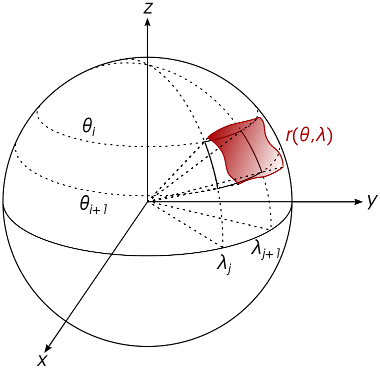

Figure: Undulated cell

$$\tilde{V}_{ij} = \frac{G\,M}{R\,\Delta\sigma_{ij}} \sum_{n=0}^{N_1} \sum_{m=0}^{n} \sum_{l=0}^{1} \bar{V}_{lnm} \int\limits_{\lambda=\lambda_j}^{\lambda_{j+1}} \int\limits_{\theta=\theta_i}^{\theta_{i+1}} \left(\frac{R}{r(\theta,\lambda)} \right)^{n+1} \bar{Y}_{lnm}(\theta,\lambda)\, \sin\theta \, \mathrm{d}\theta \, \mathrm{d}\lambda.$$

Motivation

We impose on $r(\theta, \lambda)$ to be of the form

$$r(\theta, \lambda) = \sum_{n=0}^{N_2} \sum_{m=0}^{n} \sum_{l=0}^{1} \bar{r}_{lnm} \, \bar{Y}_{lnm}(\theta, \lambda).$$

Motivation

We impose on $r(\theta, \lambda)$ to be of the form

$$r(\theta, \lambda) = \sum_{n=0}^{N_2} \sum_{m=0}^{n} \sum_{l=0}^{1} \bar{r}_{lnm} \, \bar{Y}_{lnm}(\theta, \lambda).$$

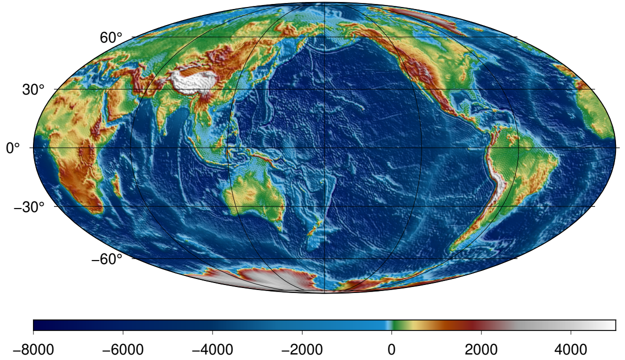

Figure: Earth's topography up to $N_2 = 360$

Motivation

We impose on $r(\theta, \lambda)$ to be of the form

$$r(\theta, \lambda) = \sum_{n=0}^{N_2} \sum_{m=0}^{n} \sum_{l=0}^{1} \bar{r}_{lnm} \, \bar{Y}_{lnm}(\theta, \lambda).$$

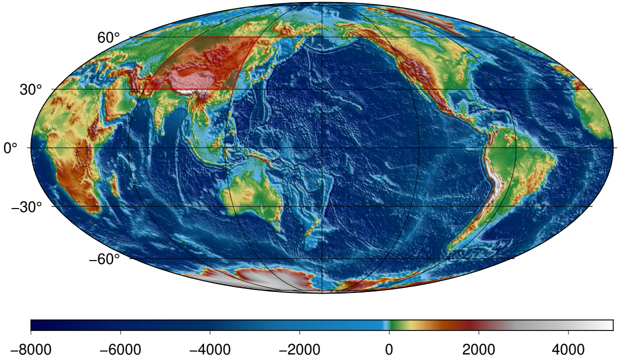

Figure: Earth's topography up to $N_2 = 360$

Method

Surface SHE of $q^{n+1}(\theta, \lambda)$

Let us expand $(R/r(\theta,\lambda))^{n+1}$ for each $n = 0, 1, \cdots, N_1$ into surface spherical harmonics,

$$\left(\frac{R}{r(\theta,\lambda)}\right)^{n+1} = q^{n+1}(\theta,\lambda) \tag{1}$$

Surface SHE of $q^{n+1}(\theta, \lambda)$

Let us expand $(R/r(\theta, \lambda))^{n+1}$ for each $n = 0, 1, \cdots, N_1$ into surface spherical harmonics,

$$\left(\frac{R}{r(\theta, \lambda)}\right)^{n+1} = q^{n+1}(\theta, \lambda) = \sum_{n'=0}^{\infty} \sum_{m'=0}^{n'} \sum_{l'=0}^{1} \bar{q}_{l'n'm'}^{(n+1)} \, \bar{Y}_{l'n'm'}(\theta, \lambda) \tag{1}$$

Surface SHE of $q^{n+1}(\theta, \lambda)$

Let us expand $(R/r(\theta, \lambda))^{n+1}$ for each $n = 0, 1, \cdots, N_1$ into surface spherical harmonics,

$$\begin{aligned}\left(\frac{R}{r(\theta,\lambda)}\right)^{n+1} &= q^{n+1}(\theta,\lambda) \\ &= \sum_{n'=0}^{\infty} \sum_{m'=0}^{n'} \sum_{l'=0}^{1} \bar{q}_{l'n'm'}^{(n+1)} \, \bar{Y}_{l'n'm'}(\theta,\lambda) \\ &\approx \sum_{n'=0}^{N_3} \sum_{m'=0}^{n'} \sum_{l'=0}^{1} \bar{q}_{l'n'm'}^{(n+1)} \, \bar{Y}_{l'n'm'}(\theta,\lambda).\end{aligned} \tag{1}$$

Surface SHE of $q^{n+1}(\theta, \lambda)$

Let us expand $(R/r(\theta,\lambda))^{n+1}$ for each $n = 0, 1, \cdots, N_1$ into surface spherical harmonics,

$$\begin{aligned}\left(\frac{R}{r(\theta,\lambda)}\right)^{n+1} &= q^{n+1}(\theta,\lambda) \\ &= \sum_{n'=0}^{\infty} \sum_{m'=0}^{n'} \sum_{l'=0}^{1} \bar{q}_{l'n'm'}^{(n+1)} \, \bar{Y}_{l'n'm'}(\theta,\lambda) \\ &\approx \sum_{n'=0}^{N_3} \sum_{m'=0}^{n'} \sum_{l'=0}^{1} \bar{q}_{l'n'm'}^{(n+1)} \, \bar{Y}_{l'n'm'}(\theta,\lambda).\end{aligned} \tag{1}$$

Does n' really go up to ∞ even for $r(\theta,\lambda)$ truncated at N_2?

Surface SHE of $q^{n+1}(\theta, \lambda)$ – Proof I

We want to show that the surface spherical harmonic expansion of $q^{n+1}(\theta, \lambda)$ is infinite for all non-negative integers n unless $r(\theta, \lambda)$ is constant.
Throughout the derivations, we assume that $r(\theta, \lambda) > 0$ for all θ and λ.
We start with the constant $r(\theta, \lambda)$, that is, $N_2 = 0$. Then, $q^{n+1}(\theta, \lambda)$ is obviously constant, too, hence it is band-limited to degree $N_3 = 0$.
Now, let $r(\theta, \lambda)$ be an undulated surface with some $N_2 > 0$. Introducing the variable

$$\Delta r(\theta, \lambda) = \max(r(\theta, \lambda)) - r(\theta, \lambda), \tag{2}$$

which satisfies

$$0 \leq \Delta r(\theta, \lambda) < \max(r(\theta, \lambda)), \tag{3}$$

we can rewrite $q^{n+1}(\theta, \lambda)$ as

$$\begin{aligned} q^{n+1}(\theta, \lambda) &= \left(\frac{r(\theta, \lambda)}{R}\right)^{-n-1} = \left(\frac{\max(r(\theta, \lambda)) - \Delta r(\theta, \lambda)}{R}\right)^{-n-1} \\ &= \left(\frac{\max(r(\theta, \lambda))}{R}\right)^{-n-1} \left[1 + \left(-\frac{\Delta r(\theta, \lambda)}{\max(r(\theta, \lambda))}\right)\right]^{-n-1} . \end{aligned} \tag{4}$$

Surface SHE of $q^{n+1}(\theta, \lambda)$ – Proof II

With

$$w(\theta, \lambda) = -\frac{\Delta r(\theta, \lambda)}{\max(r(\theta, \lambda))}, \tag{5}$$

the square bracket in Eq. (4) can be expanded into the binomial series

$$[1 + w(\theta, \lambda)]^{-n-1} = \sum_{p=0}^{\infty} \binom{-n-1}{p} w^p(\theta, \lambda), \tag{6}$$

which converges absolutely for

$$|w(\theta, \lambda)| < 1. \tag{7}$$

Combining Eqs. (4) and (6), we finally arrive at

$$q^{n+1}(\theta, \lambda) = \left(\frac{\max(r(\theta, \lambda))}{R} \right)^{-n-1} \sum_{p=0}^{\infty} \binom{-n-1}{p} w^p(\theta, \lambda). \tag{8}$$

Surface SHE of $q^{n+1}(\theta, \lambda)$ – Proof III

From Eqs. (2) and (5), it is clear that the maximum degree of $w(\theta, \lambda)$ is the same as that of $r(\theta, \lambda)$, that is, N_2. Then, it follows from Lemma 4.1 of [Freeden and Schneider(1998)] that the maximum degree of $w^p(\theta, \lambda)$ is $p \times N_2$. Since the binomial series (8) converges for all θ and λ (see Eqs. 3, 5 and 7), the asymptotic relation $p \times N_2 \to \infty$ for $p \to \infty$ proves that the surface spherical harmonic expansion of $q^{n+1}(\theta, \lambda)$ is infinite as long as $N_2 > 0$.

Surface SHE of $q^{n+1}(\theta, \lambda)$ – Numerical example

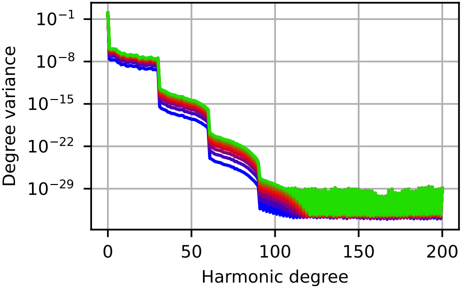

Figure: Spectra of $q^{n+1}(\theta, \lambda)$ for $n = 0$ (the blue line), 2, 4, $\cdots$, 14 (the green line) with $r(\theta, \lambda)$ being the Earth's surface expanded up to degree $N_2 = 30$. Somewhere beyond degree 90, double precision is not sufficient due to the small magnitudes of these frequencies. Quadruple precision resolves this if needed

Surface SHE of $q^{n+1}(\theta, \lambda)$ – Numerical example

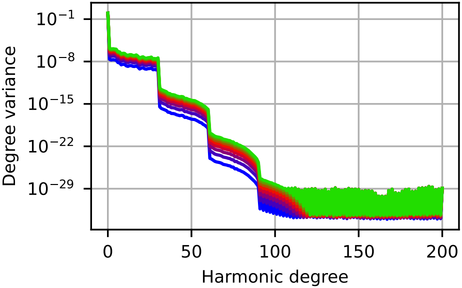

Figure: Spectra of $q^{n+1}(\theta, \lambda)$ for $n = 0$ (the blue line), 2, 4, $\cdots$, 14 (the green line) with $r(\theta, \lambda)$ being the Earth's surface expanded up to degree $N_2 = 30$. Somewhere beyond degree 90, double precision is not sufficient due to the small magnitudes of these frequencies. Quadruple precision resolves this if needed

The step-like features are explained (**not caused!**) by the binomial expansion.

Final equation I

With Eq. (1) and after some math, we get

$$\boxed{\tilde{V}_{ij} = \frac{G\,M}{R\,\Delta\sigma_{ij}} \sum_{m=0}^{N_1} \sum_{m'=0}^{N_3} \tilde{V}_{ijmm'},} \tag{9}$$

where

$$\tilde{V}_{ijmm'} = \sum_{l=0}^{1} \sum_{l'=0}^{1} \mathrm{IT}_{lm}^{l'm'}(\lambda_j, \lambda_{j+1})\, \mathrm{LC}_{lm}^{l'm'}(\theta_i, \theta_{i+1}),$$

$$\mathrm{LC}_{lm}^{l'm'}(\theta_i, \theta_{i+1}) = \sum_{k=0}^{N_1} \sum_{k'=0}^{N_3} \mathrm{IPT}_{mk}^{m'k'}(\theta_i, \theta_{i+1})\, \overline{\mathrm{VQ}}_{lmk}^{l'm'k'},$$

$$\overline{\mathrm{VQ}}_{lmk}^{l'm'k'} = \sum_{\substack{n=\max(k,m)\\(n-k):\ \text{even}}}^{N_1} \bar{V}_{lnm}\, \bar{p}_{nmk} \sum_{\substack{n'=\max(k',m')\\(n'-k'):\ \text{even}}}^{N_3} \bar{q}_{l'n'm'}^{(n+1)}\, \bar{p}_{n'm'k'}$$

Final equation II

with

$$\mathrm{IT}_{lm}^{l'm'}(\lambda_j, \lambda_{j+1}) = \int\limits_{\lambda_j}^{\lambda_{j+1}} \begin{Bmatrix} \cos(m\,\lambda)\,\cos(m'\,\lambda) & (l=0,\, l'=0) \\ \cos(m\,\lambda)\,\sin(m'\,\lambda) & (l=0,\, l'=1) \\ \sin(m\,\lambda)\,\cos(m'\,\lambda) & (l=1,\, l'=0) \\ \sin(m\,\lambda)\,\sin(m'\,\lambda) & (l=1,\, l'=1) \end{Bmatrix} \mathrm{d}\lambda,$$

$$\mathrm{IPT}_{mk}^{m'k'}(\theta_i, \theta_{i+1}) = \int\limits_{\theta_i}^{\theta_{i+1}} \begin{Bmatrix} \cos(k\,\theta)\,\cos(k'\,\theta) & (m\colon \text{even},\, m'\colon \text{even}) \\ \cos(k\,\theta)\,\sin(k'\,\theta) & (m\colon \text{even},\, m'\colon \text{odd}) \\ \sin(k\,\theta)\,\cos(k'\,\theta) & (m\colon \text{odd},\, m'\colon \text{even}) \\ \sin(k\,\theta)\,\sin(k'\,\theta) & (m\colon \text{odd},\, m'\colon \text{odd}) \end{Bmatrix} \sin\theta \mathrm{d}\theta$$

and $\bar{p}_{nmk}$ being the Fourier coefficients of Legendre functions.

The $\overline{\mathrm{VQ}}_{lmk}^{l'm'k'}$ coefficients resemble coefficients of a Fourier series in that they are independent of evaluation cells σ_{ij}.

Numerical experiments

Area-mean values on the Earth's surface

- Disturbing potential from EGM2008 up to $N_1 = 15$
- Earth's surface from Earth2014 up to $N_2 = 30$
- Global grid of $N_\theta = 180$ and $N_\lambda = 360$ cells
- Reference values from numerical integration
  Single reference area-mean value from 250×250 point values
  ($\sim 10^9$ in total, quadruple precision)

Area-mean values on the Earth's surface

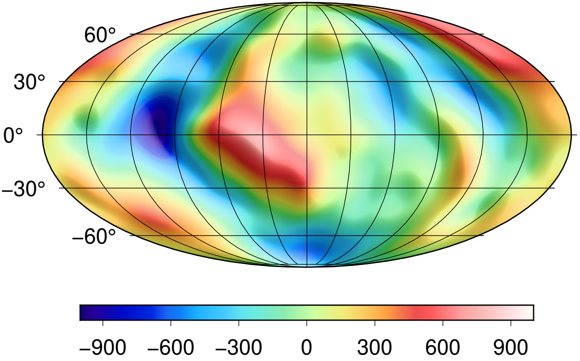

Figure: Reference area-mean disturbing potential from the numerical integration ($\mathrm{m}^2\ \mathrm{s}^{-2}$). The potential is evaluated up to degree $N_1 = 15$ on the Earth's surface expanded up to $N_2 = 30$. The computational cells are organized at a global equiangular grid of 1° cells

Area-mean values on the Earth's surface

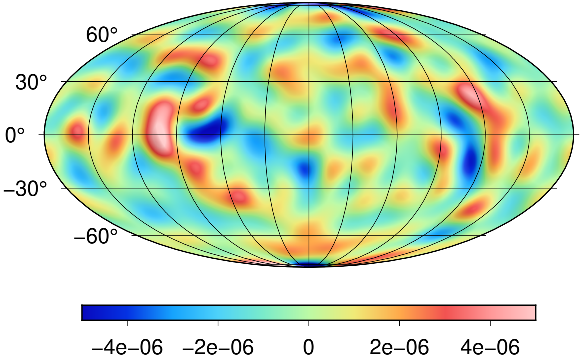

Figure: Differences between the new method and the reference data ($m^2\ s^{-2}$). The statistics of the differences are: min $= -8.5 \times 10^{-5}$, max $= 8.7 \times 10^{-5}$, mean $= 3.0 \times 10^{-8}$, STD $= 5.7 \times 10^{-6}$; all values in $m^2\ s^{-2}$. The maximum degree of $N_3 = 200$ was used to truncate all harmonic series of $q^{n+1}(\theta, \lambda)$

The discrepancies reflect mostly the errors of the *reference* data.

Convergence/divergence on planetary topographies

- Gravitational potential to $N_1 = 100$ (from spectral forward modelling)
- Bennu's surface to $N_2 = 15$
- Global grid of $N_\theta = 150$ and $N_\lambda = 300$ cells
- Reference data from spatial-domain gravity forward modelling method after [Fukushima(2017)] ($\sim$10 correct digits)

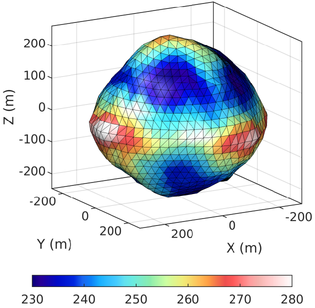

Figure: (101955) Bennu

Convergence/divergence on planetary topographies

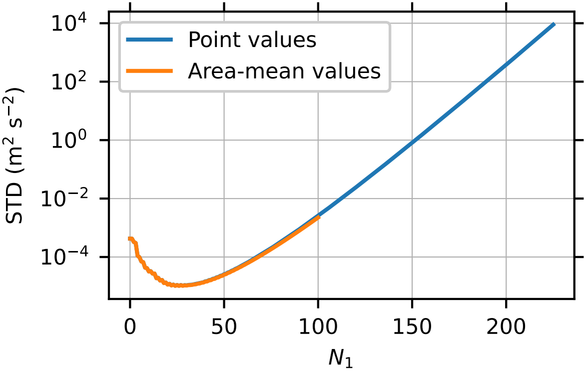

Figure: Series behaviour of point and area-mean values on the surface of Bennu

CHarm

CHarm

CHarm is a C library to perform spherical harmonic tranforms up to high degrees.

CHarm

CHarm is a C library to perform spherical harmonic tranforms up to high degrees.

Main features:

- FFT-based surface SHA and solid SHS

CHarm

CHarm is a C library to perform spherical harmonic tranforms up to high degrees.

Main features:

- FFT-based surface SHA and solid SHS
- Stable up to high degrees (tens of thousands and beyond)

CHarm

CHarm is a C library to perform spherical harmonic tranforms up to high degrees.

Main features:

- FFT-based surface SHA and solid SHS
- Stable up to high degrees (tens of thousands and beyond)
- Single, double and **quadruple** precision

CHarm

CHarm is a C library to perform spherical harmonic tranforms up to high degrees.

Main features:

- FFT-based surface SHA and solid SHS
- Stable up to high degrees (tens of thousands and beyond)
- Single, double and **quadruple** precision
- Works with point and area-mean data values (both SHA and SHS)

CHarm

CHarm is a C library to perform spherical harmonic tranforms up to high degrees.

Main features:

- FFT-based surface SHA and solid SHS
- Stable up to high degrees (tens of thousands and beyond)
- Single, double and **quadruple** precision
- Works with point and area-mean data values (both SHA and SHS)
- Etcetera, etcetera

CHarm

CHarm is a C library to perform spherical harmonic tranforms up to high degrees.

Main features:

- FFT-based surface SHA and solid SHS
- Stable up to high degrees (tens of thousands and beyond)
- Single, double and **quadruple** precision
- Works with point and area-mean data values (both SHA and SHS)
- Etcetera, etcetera
- Discrete FFT by FFTW

CHarm

CHarm is a C library to perform spherical harmonic tranforms up to high degrees.

Main features:

- FFT-based surface SHA and solid SHS
- Stable up to high degrees (tens of thousands and beyond)
- Single, double and **quadruple** precision
- Works with point and area-mean data values (both SHA and SHS)
- Etcetera, etcetera
- Discrete FFT by FFTW
- OpenMP parallelization for shared-memory architectures

CHarm – Source Code

- Source code: `https://github.com/blazej-bucha/charm`
  Releases in `master`
  Development in `develop`
- Tarball and zip files of releases:
  `https://github.com/blazej-bucha/charm/tags`
- Unrestrictive 3-clause BSD license
- You may also visit `https://blazejbucha.com` for other codes

CHarm – Documentation

https://blazej-bucha.github.io/charm/index.html

0.0.0

Search docs

Introduction
Installing
Some definitions to make things clear
Cookbook
Modules
charm_shc
charm_crd
charm_shs
charm_sha
charm_leg
charm_integ
charm_misc
charm_xnum
charm_err
charm_glob
charm
Benchmarks
Tested platforms
Citing
License

`charm_shc *charm_shc_init(unsigned long nmax, double mu, double r)`

Allocates and initializes a `charm_shc` structure of spherical harmonic coefficients up to the degree `nmax`. All coefficients are initialized to zero and are associated with the scaling parameter `mu` and the radius of the reference sphere `r`.

On success, returned is a pointer to the `charm_shc` structure. On error, `NULL` is returned.

Warning

The `charm_shc` structure created by this function must be deallocated by calling `charm_shc_free`. The `free` function will *not* deallocate the memory and will lead to memory leaks.

Note

`r` must be greater than zero.

`void charm_shc_free(charm_shc *shcs)`

Frees the memory associated with `shcs`. No operation is performed if `shcs` is `NULL`.

`void charm_shc_read_bin(FILE *stream, unsigned long nmax, charm_shc *shcs, charm_err *err)`

Reads a `charm_shc` structure to `shcs` from a binary file pointed to by `stream`. The structure is loaded up to the maximum spherical harmonic degree `nmax`. The file is assumed to has been created by `charm_shc_write_bin` on the same architecture. Error reported by the function (if any) is written to `err`.

The input file is a binary representation of the `charm_shc` structure in the following order:

$$\begin{aligned}&\text{nmax2},\ \mu,\ R, \bar{C}_{0,0}, \bar{C}_{1,0}, \bar{C}_{2,0}, \cdots, \bar{C}_{\text{nmax2},0}, \bar{C}_{1,1}, \bar{C}_{2,1}, \cdots,\\ &\bar{C}_{\text{nmax2},1}, \bar{C}_{2,2}, \bar{C}_{3,2}, \cdots, \bar{C}_{\text{nmax2},\text{nmax2}}, \bar{S}_{0,0}, \bar{S}_{1,0}, \bar{S}_{2,0}, \cdots,\\ &\bar{S}_{\text{nmax2},0}, \bar{S}_{1,1}, \bar{S}_{2,1}, \cdots, \bar{S}_{\text{nmax2},1}, \bar{S}_{2,2}, \bar{S}_{3,2}, \cdots, \bar{S}_{\text{nmax2},\text{nmax2}},\end{aligned}$$

where `nmax2` is the maximum harmonic degree related to the `charm_shc` structure stored in the file,

$$\mu, R$$

are the scaling parameter of the coefficients and the associated radius of the reference sphere

Conclusions

Conclusions

- New method to integrate solid SHEs on undulated surfaces developed

Conclusions

- New method to integrate solid SHEs on undulated surfaces developed
- Suitable mostly for medium-degree harmonic expansions

Conclusions

- New method to integrate solid SHEs on undulated surfaces developed
- Suitable mostly for medium-degree harmonic expansions
- Similar convergence properties as for point values

Conclusions

- New method to integrate solid SHEs on undulated surfaces developed
- Suitable mostly for medium-degree harmonic expansions
- Similar convergence properties as for point values
- Can be used in the *Change of Boundary Approach* to downward continue area-mean values more accurately

Conclusions

- New method to integrate solid SHEs on undulated surfaces developed
- Suitable mostly for medium-degree harmonic expansions
- Similar convergence properties as for point values
- Can be used in the *Change of Boundary Approach* to downward continue area-mean values more accurately
- Easy to extend to radial derivatives of the potential

Conclusions

- New method to integrate solid SHEs on undulated surfaces developed
- Suitable mostly for medium-degree harmonic expansions
- Similar convergence properties as for point values
- Can be used in the *Change of Boundary Approach* to downward continue area-mean values more accurately
- Easy to extend to radial derivatives of the potential
- A C library to perform harmonic transforms up to high degrees released

References

W. Freeden and F. Schneider.
Wavelet approximations on closed surfaces and their application to boundary-value problems of potential theory.
Mathematical Methods in the Applied Sciences, 21:129–163, 1998.

T. Fukushima.
Precise and fast computation of the gravitational field of a general finite body and its application to the gravitational study of asteroid Eros.
The Astronomical Journal, 154(145):15pp, 2017.
doi: 10.3847/1538-3881/aa88b8.

Thank you for your attention!

CHarm is available at:

- `https://github.com/blazej-bucha/charm`
- `https://blazejbucha.com`

Backup slides

Motivation

Spherical cell with constant r:

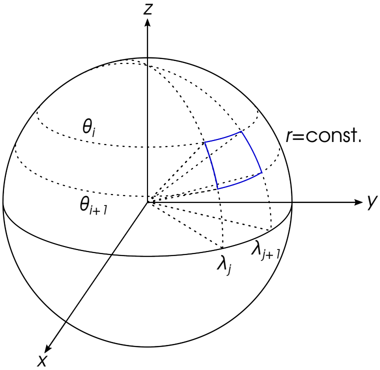

Figure: Spherical cell

Motivation

Spherical cell with constant r:

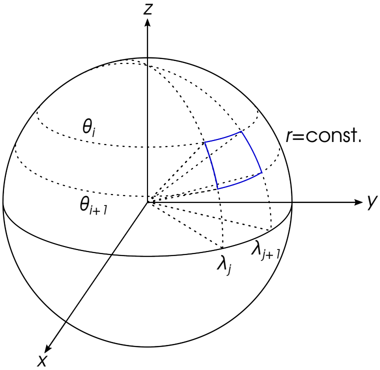

Figure: Spherical cell

$$\tilde{V}_{ij} = \frac{G\,M}{R\,\Delta\sigma_{ij}} \sum_{n=0}^{N_1} \left(\frac{R}{r}\right)^{n+1} \sum_{m=0}^{n} \sum_{l=0}^{1} \bar{V}_{lnm} \int\limits_{\lambda=\lambda_j}^{\lambda_{j+1}} \int\limits_{\theta=\theta_i}^{\theta_{i+1}} \bar{Y}_{lnm}(\theta,\lambda)\, \sin\theta \, \mathrm{d}\theta \, \mathrm{d}\lambda.$$

Area-mean values on a sphere

- Disturbing potential from EGM2008:

$$T(r,\theta,\lambda) = \frac{G\,M}{R} \sum_{n=0}^{N_1} \left(\frac{R}{r}\right)^{n+1} \sum_{m=0}^{n} \sum_{l=0}^{1} \bar{T}_{lnm}\,\bar{Y}_{lnm}(\theta,\lambda). \tag{10}$$

- Earth's surface from Earth2014 TBI up to $N_2 = 0$:

$$r(\theta,\lambda) = \bar{r}_{000}. \tag{11}$$

  Therefore, $N_3 = 0$ and the new method is exact.

- Reference values using the known synthesis of area-mean values on a sphere (quadruple precision).

Area-mean values on a sphere

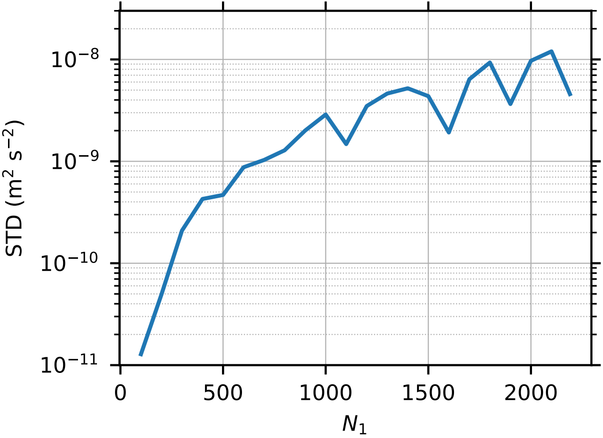

Figure: Standard deviation (STD) of the discrepancies between the new and the reference method on a sphere ($N_2 = 0$) as a function of the maximum harmonic degree of the disturbing potential, $N_1 = 100, 200, \ldots, 2100, 2190$. The tests were performed at global grids with $N_\theta = N_1 + 1$ and $N_\lambda = 2N_\theta$ cells of equal size in the co-latitudinal and longitudinal directions, respectively

Numerical implementation

How to compute Eq. (9) in grids?

Numerical implementation

How to compute Eq. (9) in grids?

Either

with *little memory* requirements but painfully **slow**

or

reasonably **fast** but with *huge memory* requirements.

Numerical implementation

How to compute Eq. (9) in grids?

Either

with *little memory* requirements but painfully **slow**

or

$\boxed{\text{reasonably \textbf{fast} but with \textit{huge memory} requirements.}}$

Assuming double precision and 8 bytes per coefficient, $\overline{\mathrm{VQ}}_{lmk}^{l'm'k'}$ occupy $4(N_1+1)^2(N_3+1)^2\,8/1024^3$ GBs of memory:

- $\sim$3 GBs of memory are needed for $N_1 = N_3 = 100$,
- $\sim$49 GBs of memory are needed for $N_1 = N_3 = 200$,
- $\sim$245 GBs of memory are needed for $N_1 = N_3 = 300$.

Area-mean values on the Earth's surface – effect of N_3

- Disturbing potential to $N_1 = 100$
- Earth's surface to $N_2 = 100$
- Global grid of $N_\theta = 600$ and $N_\lambda = 1200$ cells
- Reference data from the new method with $N_3 = 600$

Area-mean values on the Earth's surface – effect of N_3

- Disturbing potential to $N_1 = 100$
- Earth's surface to $N_2 = 100$
- Global grid of $N_\theta = 600$ and $N_\lambda = 1200$ cells
- Reference data from the new method with $N_3 = 600$

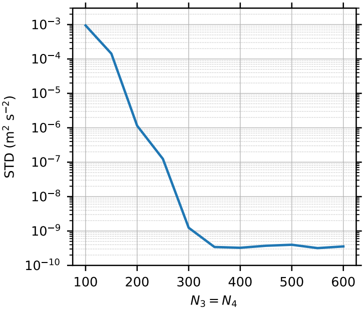

Figure: Accuracy of the new method for $N_3 = N_4 = 100, 150, \ldots, 600$ with $N_1 = N_2 = 100$ fixed. All solutions are validated against a reference one ($N_3 = 600$ and $N_4 = 1600$) in terms of the standard deviation (STD) of the discrepancies.

Computation time

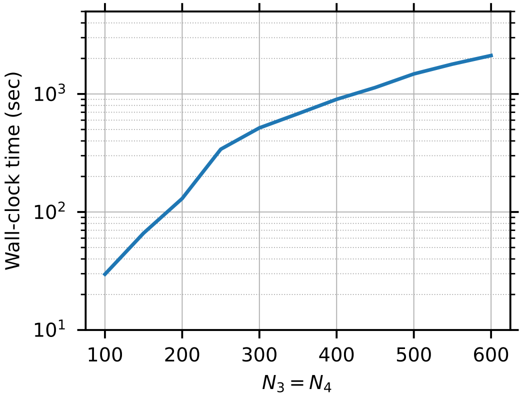

Figure: Wall-clock time needed to evaluate the data for previous figure. The experiments were performed on a PC with Intel(R) Core(TM) i7-6800K CPU @ 3.40GHz and 128 GBs of RAM running under Debian GNU/Linux v. 11.1. CHarm was compiled with the GNU compiler collection v. 10.2.1 using the `-O3` optimization flag and with the OpenMP parallelization enabled. All 12 threads of the CPU were employed.

CHarm

CHarm – Accuracy (Closed-Loop Experiments)

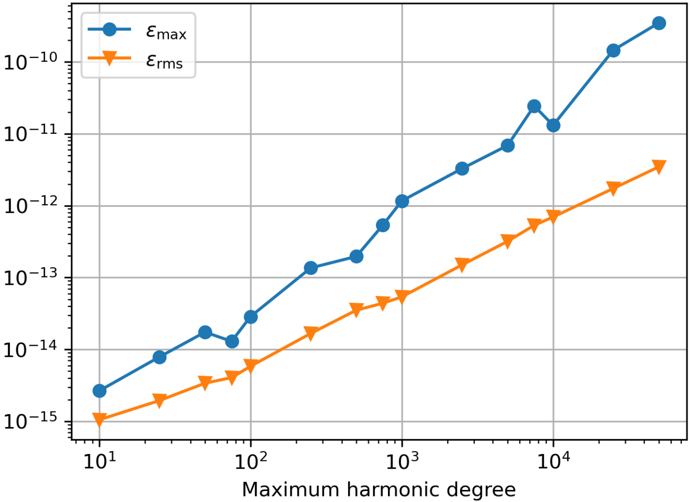

CHarm – Speed

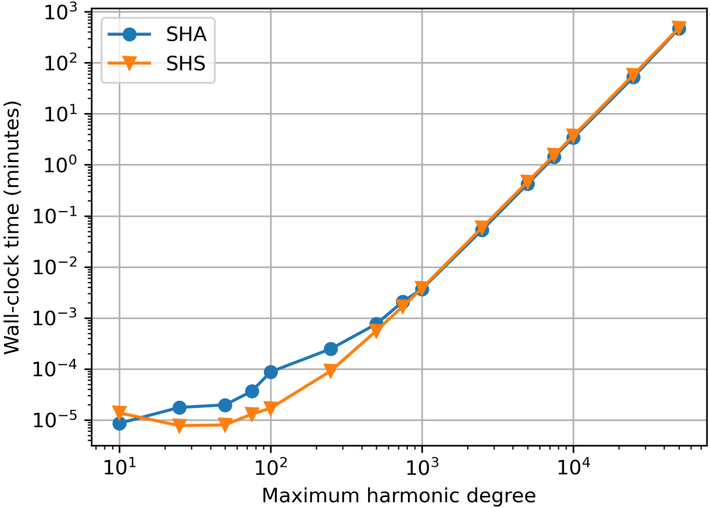
SHA
SHS
Wall-clock time (minutes)
Maximum harmonic degree
10^{3}
10^{2}
10^{1}
10^{0}
10^{-1}
10^{-2}
10^{-3}
10^{-4}
10^{-5}
10^{1}
10^{2}
10^{3}
10^{4}